

## Transdimensional inference for gravitational-wave astronomy with Bilby

HUI TONG,<sup>1,2</sup> NIR GUTTMAN,<sup>1,2</sup> TEAGAN A. CLARKE,<sup>1,2</sup> PAUL D. LASKY,<sup>1,2</sup> ERIC THRANE,<sup>1,2</sup> ETHAN PAYNE,<sup>3,4</sup>  
ROWINA NATHAN,<sup>1,2</sup> BEN FARR,<sup>5</sup> MAYA FISHBACH,<sup>6,7,8</sup> GREGORY ASHTON,<sup>9</sup> AND VALENTINA DI MARCO<sup>1,2</sup>

<sup>1</sup>*School of Physics and Astronomy, Monash University, Vic 3800, Australia*

<sup>2</sup>*OzGrav: The ARC Centre of Excellence for Gravitational Wave Discovery, Clayton VIC 3800, Australia*

<sup>3</sup>*Department of Physics, California Institute of Technology, Pasadena, California 91125, USA*

<sup>4</sup>*LIGO Laboratory, California Institute of Technology, Pasadena, California 91125, USA*

<sup>5</sup>*Institute for Fundamental Science, Department of Physics, University of Oregon, Eugene, OR 97403, USA*

<sup>6</sup>*Canadian Institute for Theoretical Astrophysics, 60 St George St, University of Toronto, Toronto, ON M5S 3H8, Canada*

<sup>7</sup>*David A. Dunlap Department of Astronomy and Astrophysics, 50 St George St, University of Toronto, Toronto, ON M5S 3H8, Canada*

<sup>8</sup>*Department of Physics, 60 St George St, University of Toronto, Toronto, ON M5S 3H8, Canada*

<sup>9</sup>*Department of Physics, Royal Holloway, University of London, TW20 0EX, UK*

### ABSTRACT

It has become increasingly useful to answer questions in gravitational-wave astronomy using *transdimensional* models where the number of free parameters can be varied depending on the complexity required to fit the data. Given the growing interest in transdimensional inference, we introduce a new package for the Bayesian inference Library (Bilby) called `tBilby`. The `tBilby` package allows users to set up transdimensional inference calculations using the existing Bilby architecture with off-the-shelf nested samplers and/or Markov Chain Monte Carlo algorithms. Transdimensional models are particularly helpful when we seek to test theoretically uncertain predictions described by phenomenological models. For example, bursts of gravitational waves can be modelled using a superposition of  $N$  wavelets where  $N$  is itself a free parameter. Short pulses are modelled with small values of  $N$  whereas longer, more complicated signals are represented with a large number of wavelets stitched together. Other transdimensional models have found use describing instrumental noise and the population properties of gravitational-wave sources. We provide a few demonstrations of `tBilby`, including fitting the gravitational-wave signal GW150914 with a superposition of  $N$  sine-Gaussian wavelets. We outline our plans to further develop the `tBilby` code suite for a broader range of transdimensional problems.

### 1. INTRODUCTION

Since the first detection of gravitational waves (Abbott et al. 2016a), Bayesian inference has been widely used to infer the astrophysical properties of merging binaries (Abbott et al. 2016b). Bayesian inference is used to search for physics beyond general relativity (Abbott et al. 2016c), to probe nuclear physics at extreme densities (Abbott et al. 2018), to measure the expansion of the Universe (Abbott et al. 2017; Hotokezaka et al. 2019), and to study the formation of merging binaries (Abbott et al. 2021, 2023).

In many applications, the framework underpinning these inferences is theoretically precise; that is, we have trustworthy, quantitative predictions for the data given

the model parameters. For example, when we infer the masses of merging black holes, we are able to leverage state-of-the-art gravitational waveforms, built from numerical-relativity simulations, to interpret data. In other cases, however, there is significant theoretical uncertainty and so we rely on phenomenological models. For example, following the detection of GW150914, the LIGO–Virgo Collaborations used the `BayesWave` algorithm (Cornish & Littenberg 2015) to perform a study to reconstruct the strain time series in the data with minimal assumptions using a superposition of  $N$  sine-Gaussian wavelets (Abbott 2016; Klimentenko et al. 2008).<sup>1</sup> If we treat  $N$  as a free parameter, then the total number of model parameters is itself variable. Such an analysis—where the number of free parameters is it-

Corresponding author: Hui Tong  
[hui.tong@monash.edu](mailto:hui.tong@monash.edu)

<sup>1</sup> Sine-Gaussian functions are sometimes called Morlet or Gabor wavelets (Kronland-Martinet et al. 1987)

self a free parameter—is said to be *transdimensional*. The striking agreement between LIGO–Virgo’s minimal-assumption reconstruction and the waveform predicted by general relativity helped cement the interpretation of the signal as a binary black hole merger (Abbott 2016). It remains a powerful demonstration of the usefulness of transdimensional models.

There are other noteworthy applications of transdimensional inference in gravitational-wave astronomy. In the audio band where the LIGO–Virgo–KAGRA (LVK; Aasi et al. 2015; Acernese et al. 2015; Aso et al. 2013) observatories operate, the **BayesWave** package (Cornish & Littenberg 2015; Cornish et al. 2021) has been used for minimum-assumption model checking and waveform reconstruction (Millhouse et al. 2018; Pannarale et al. 2021; Dàya et al. 2021), improving the statistical significance of short and unmodeled “bursting” signals (Littenberg et al. 2016; Yi Shuen C. Lee & Melatos 2021), modelling astrophysically uncertain waveforms (e.g., from supernovae and hypermassive neutron stars) (Raza et al. 2022; Miravet-Tenés et al. 2023; Ashton & Dietrich 2022), modelling deviations from general relativity (Chatziioannou et al. 2021b; Johnson-McDaniel et al. 2022), and subtracting noise artifacts (glitches) (Littenberg & Cornish 2010; Pankow et al. 2018; Chatziioannou et al. 2021a; Davis et al. 2022; Hourihane et al. 2022). Meanwhile, the related **BayesLine** code is frequently used to estimate the noise power spectral density of gravitational-wave measurements (Littenberg & Cornish 2015; Gupta & Cornish 2023). Transdimensional analyses have also been demonstrated for use in the millihertz band by space-based observatories (Littenberg et al. 2020) and in the nanohertz band by pulsar timing arrays (Ellis & Cornish 2016). The code package **Eryn** (Karnesis et al. 2023) was recently introduced as a multi-purpose tool for transdimensional inference with special attention to problems relevant for the LVK and LISA.

In this work, we introduce **tBilby**, a package for transdimensional sampling with the Bayesian Inference Library **Bilby** (Ashton et al. 2019; Romero-Shaw et al. 2020). **Bilby** is widely used in gravitational-wave astronomy. It is designed and maintained with four guiding principles: modularity, consistency, generality, and usability. The mission for **Bilby** is to be intuitive enough to be used by new researchers, while still being applicable to a broad class of problems, and with the ability to easily swap samplers when needed. Our goal is to leverage these attributes, building on the existing **Bilby** infrastructure, in order to make it easier for **Bilby** users to carry out transdimensional analyses.

We envision the **tBilby** project as a long-term effort that will be developed gradually. With this in mind, we start here with a specific class of transdimensional problems: transient waveforms that can be modelled with a superposition of  $N$  component functions. In particular, we demonstrate a minimum-assumption reconstruction of GW150914 using a superposition of  $N$  sine-Gaussian functions. We use this demonstration to explain key concepts in transdimensional inference including the notion of ghost parameters and proximity priors (see Section 2 for more details). Readers can reproduce our calculation using the accompanying code.<sup>2</sup> The remainder of this paper is organized as follows. In Section 2, we cover the basic principles of transdimensional inference and describe how they are implemented in **tBilby**. In Section 3, we demonstrate the **tBilby** package with two examples: a toy-model problem consisting of a superposition of Gaussian pulses and a minimum-assumption reconstruction of GW150914. We provide closing remarks in Section 4, briefly demonstrating another transdimensional example fitting LIGO’s noise amplitude spectral density with a sum of  $N$  power laws and  $M$  Lorentzian functions. We also sketch our priorities for future development.

## 2. METHOD

One of the goals of Bayesian inference is to determine the posterior distribution for model parameters  $\vec{\theta}$  given a prior  $\pi(\vec{\theta})$ , data  $d$ , and likelihood  $\mathcal{L}(d|\vec{\theta})$ . In a transdimensional problem, the number of parameters  $N$  is itself a parameter:

$$\vec{\theta} \equiv \{\theta_1, \dots, \theta_N, N\}. \quad (1)$$

In some cases, this problem can be solved with brute-force parallelization: one can run multiple inference jobs, each with a different *fixed* number of parameters  $N$ , and then combine the resulting samples based on the Bayesian evidence for each fixed- $N$  analysis  $\mathcal{Z}_N$ , as well as their prior preference. This approach works adequately when there is a relatively small range of values for  $N$ . However, it becomes inefficient when time is wasted exploring many values of  $N$  disfavoured by the likelihood function. The solution is to sample in  $N$ .<sup>3</sup>

The number of parameters  $N$  is treated similarly to any other discrete parameter in **Bilby**. In our demonstrations below, we take the prior  $\pi(N)$  to be uniform on the interval  $[N_{\min}, N_{\max}]$ . At each step, the sampler

<sup>2</sup> The code can be found at the git repository <https://github.com/tBilby/tBilby>.

<sup>3</sup> In the context of Markov chain Monte Carlo samplers, this is essentially the same as the Reversible jump Markov chain Monte Carlo technique (Green 1995).

draws a value of  $N$  along with values for all possible parameters in  $\vec{\theta}$ —even parameters  $\theta_{k>N}$  that are not used for the  $N$ -parameter model. We refer to the  $\theta_{k>N}$  parameters as “ghost parameters” since they are not included in the likelihood evaluation, similar method to Liu et al. (2023). In App. B, we prove that when we marginalize over ghost parameters, we obtain the same posterior as one would obtain without ghost parameters using either the brute-force method or transdimensional sampler.<sup>4</sup>

From the perspective of the `tBilby` code, the transdimensional model behaves like a fixed-dimensional model in order to obtain the joint posterior:

$$p(\theta_1, \dots, \theta_{N_{\max}}, N | d) \propto \pi(\theta_1, \dots, \theta_{N_{\max}}) \pi(N) \mathcal{L}(d | \theta_1, \dots, \theta_N). \quad (2)$$

Since the likelihood does not depend on the ghost parameters, the marginal posterior distribution for the  $k > N$  ghost parameters is equivalent to the prior for the ghost parameters

$$p(\theta_k | d, N, k > N, \theta_{j \leq N}) = \pi(\theta_k | \theta_{j \leq N}). \quad (3)$$

The  $k > N$  ghost-parameter samples are removed in post-processing since they are not actually part of our model. The ghost-parameter framework is convenient since it allows us to perform transdimensional inference using the off-the-shelf samplers already available in `Bilby`.<sup>5</sup>

In this Paper, we mainly focus on a specific set of transdimensional problems in which the data consists of a time series  $d(t)$ , and the signal model  $s(t)$  is modelled with a sum of  $N$  components, each with parameters  $\theta_k$ :

$$s(t | \vec{\theta}) = \sum_{k=1}^N s_k(t | \theta_k). \quad (4)$$

We refer to each  $s_k(t | \theta_k)$  as a *component function*. There are two issues that arise when trying to stitch together component functions to reconstruct a transient signal. First, one needs to make sure the component functions are in some sense near one another so that they will add together to create a more complicated signal. If the component functions are too far apart, they do not sum to a more complex signal, instead forming distinct signals. At the same time, we do not want the component

functions to be so close that we are essentially counting the same component function more than once.

We address these issues using *proximity priors* from `BayesWave` (Cornish & Littenberg 2015). Proximity priors provide a means of making sure that component functions are placed preferentially close to—but not too close to—other component functions. While proximity priors are not an essential ingredient for transdimensional inference in general, they are often useful for problems with component functions. The optimal choice of proximity prior is problem-dependent. Choosing a suitable proximity prior is one part in the design of a transdimensional model. In the next Section, we demonstrate the principles outlined in this section with examples.

### 3. DEMONSTRATION

#### 3.1. A superposition of Gaussian pulses

As a warm-up exercise, we consider a simple problem of fitting data with  $N$  Gaussian pulses in the presence of Gaussian white noise.<sup>6</sup> Our data  $d(t)$  is a time series consisting of signal  $s(t)$  and noise  $n(t)$ :

$$d(t) = s(t) + n(t). \quad (5)$$

Our signal model is a superposition of component functions given by

$$s(t | \mu_k, A_k, \sigma_k) = \frac{A_k}{\sigma_k \sqrt{2\pi}} \exp\left(-\frac{(t - \mu_k)^2}{2\sigma_k^2}\right). \quad (6)$$

The mean  $\mu_k$ , amplitude  $A_k$  and the width  $\sigma_k$  are free to vary.

Our prior for the number of pulses  $N$  is a discrete uniform distribution  $\mathcal{U}(0, 6)$ . The prior for the location of the first pulse  $\mu_{k=1}$  is uniform over the domain of sampling times  $\mathcal{U}(0, 150)$ . The prior for the  $k^{\text{th}}$  pulse is a uniform on the interval  $\mathcal{U}(\mu_{k-1}, 150)$ . This choice of prior ensures that the pulses are all ordered in time, but it is not a proximity prior enforcing any requirement for the closeness of neighboring pulses; we add that feature in the next subsection. For the amplitudes and widths, we employ a uniform priors in the range of  $[0.5, 1.5]$  and  $[5, 20]$  respectively. We create simulated data with a signal consisting of  $N = 3$  pulses plus Gaussian white noise  $n(t)$  with variance

$$\sigma_n = \sqrt{\langle n(t)n(t') \rangle} = 0.15 \delta_{tt'}. \quad (7)$$

The likelihood is

$$\mathcal{L}(d | s, \sigma_n) = \prod_i \frac{1}{\sqrt{2\pi\sigma_n^2}} \exp\left(-\frac{(d(t_i) - s(t_i))^2}{2\sigma_n^2}\right) \quad (8)$$

<sup>4</sup> It is interesting to note that ghost parameters  $\theta_{k>N}$  incur no Occam penalty. Since the ghost parameters do not appear in the likelihood, the flexibility of the model has not changed, and so there is no penalty for adding unnecessary complexity.

<sup>5</sup> The additional computational cost incurred by drawing prior samples that we do not use is (for most applications that we foresee) negligible compared the cost of the likelihood evaluation.

<sup>6</sup> The calculations in this subsection are performed in the accompanying `jupyter` notebook, `pulse.ipynb`, in the git repository linked above.

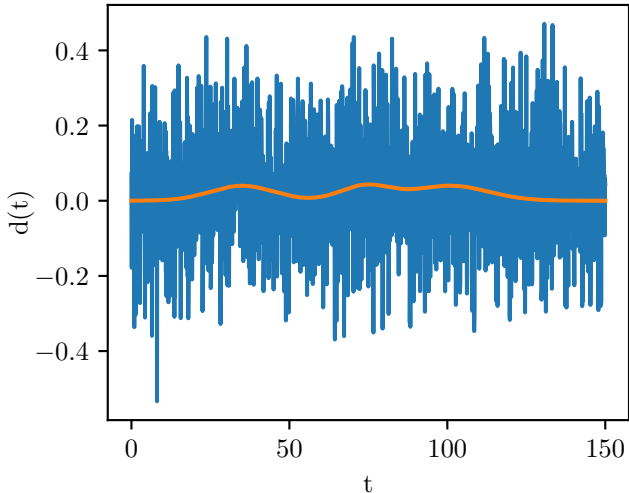


**Figure 1.** Simulated data (blue) for our Gaussian pulse model described in Subsection 3.1. The signal (orange) consists of three Gaussian pulses.

Pulse	Mean	Amplitude	Width
1	35	1.0	10
2	74	0.8	8
3	101	1.2	12

**Table 1.** Parameter values for the Gaussian pulses shown in Fig.1.

where  $d$  is data,  $s$  is signal template,  $t_i$  is a discrete time, and  $\sigma_n$  is the noise. We show simulated data in Fig. 1 created with parameters summarized in Table 1.

We run `tBilby` using two different samplers: the nested sampler `dynesty` (Speagle 2020) and the parallel-tempered Markov chain Monte Carlo sampler `ptemcee` (Vousden et al. 2015). For `ptemcee`, we update the number of pulses  $N$  and the parameters for each pulse  $\theta_k$  separately every time a new move is proposed in the sampling process. Since we are using ghost parameters, the sampler behaves as though it is exploring a fixed-dimensional space. In each iteration, we randomly add a pulse, remove a pulse, or keep fixed the number of pulses with equal probability. Since `dynesty` draws samples from priors, jumps in  $N$  occur automatically by virtue of the discrete prior  $\pi(N)$ .

In Fig. 2, we plot the posterior odds

$$\mathcal{O}(N) = \frac{\mathcal{L}(d|N)}{\mathcal{L}(d|N'=3)}, \quad (9)$$

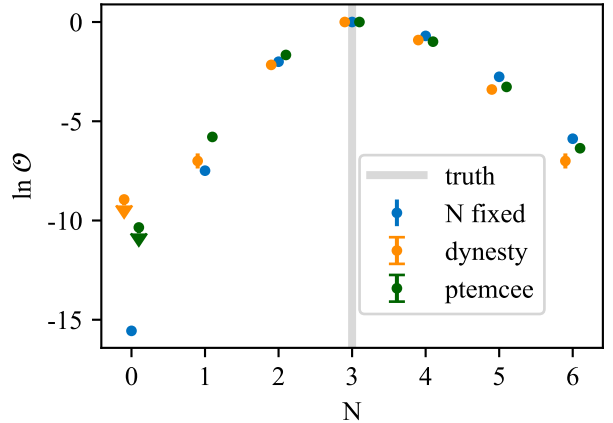


**Figure 2.** Natural log posterior odds obtained with different sampling techniques (see Eq. 9). The odds are measured relative to the favored  $N = 3$  model. The uncertainties are one-sigma. The orange and green points are transdimensional sampling results using `dynesty` and `ptemcee`. The navy blue points labelled by “N fixed” where we calculate the evidence for each value of  $N$  with dedicated `dynesty` runs provide the ground truth.

which compares the posterior support for different values of  $N$  to the best-fit  $N = 3$  model.<sup>78</sup> The results obtained with `dynesty` are shown in orange while the results obtained with `ptemcee` are shown in green. As a sanity check, we also use `dynesty` to calculate the marginal likelihood for each value of  $N$  with separate fixed- $N$ , which, combined with our prior of  $N$ , we use to estimate the ground-truth posterior obtained without transdimensional inference. All three methods produce a similar distribution. Some values of  $N$  are strongly disfavored, and so the transdimensional sample records no posterior samples for that value of  $N$ . In such cases, we set an upper limit on  $\ln \mathcal{O}$ . Both `dynesty` and `ptemcee` produce  $\ln \mathcal{O}$  values that are consistent with the fixed- $N$  ground truth.

We compare the computational cost between the brute-force method of performing many fixed- $N$  runs and using `tBilby`. The fixed- $N$  runs for  $N \in [0, 6]$

<sup>7</sup> Astute readers may notice that the right-hand side of Eq. 9 does not include the prior odds. This is because the prior odds in this case are unity.

<sup>8</sup> We estimate the uncertainty in our  $\ln \mathcal{O}$  calculations as follows:

$$\sigma_{\ln \mathcal{O}}^2 = \frac{1}{n_N} + \frac{1}{n_\phi}. \quad (10)$$

Here,  $n_N$  is the number of posterior samples for the hypothesis that the data are described by  $N$  component functions while  $n_\phi$  is the number of posterior samples describing the fiducial model—in this case,  $N = 3$ .

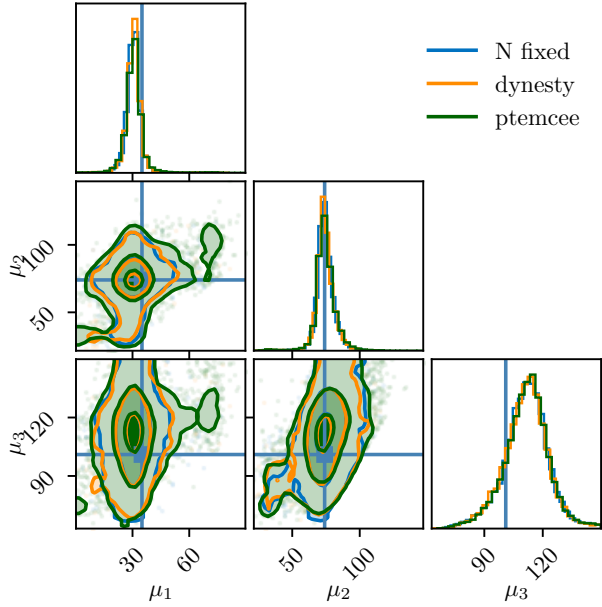


**Figure 3.** Posterior distribution for the means of  $N = 3$  Gaussian pulses. The different shades show one, two, and three-sigma credible intervals. The ground truth, obtained with a fixed- $N$  `dynesty` run, is shown in blue. In orange we plot the results obtained using a transdimensional implementation of `dynesty` while green shows a transdimensional implementation of `ptemcee`.

take roughly 4.6 times the sampling time of the `tBilby` `dynesty` run with the same sampler settings.<sup>9</sup> As expected, when we run different  $N$  models separately, most computation time is spent exploring complicated models with large  $N$ , which may not be the models with the highest Bayes factor. Since transdimensional sampling accounts for the Occam factor during sampling process, it automatically prevents the sampler exploring disfavoured regions of the parameter space.

In Fig. 3, we present a corner plot showing the marginal posterior distribution of parameters  $\mu_1, \mu_2, \mu_3$  given samples  $N = 3$ . As above, the fixed- $N$  ground truth is shown in blue while the results obtained with `dynesty` and `ptemcee` are shown in orange and green, respectively. All three posteriors produce consistent credible intervals.

### 3.2. GW150914

<sup>9</sup> Note this is not a rigorous apples-to-apples comparison. For example, we do not require the same number of effective samples between the brute-force calculation and `tBilby`. However, it does provide a rough estimate of the improvement in computational cost for this particular problem.

We now apply transdimensional inference to reconstruct the signal from the first gravitational-wave observation GW150914<sup>10</sup>. Following `BayesWave` (Cornish & Littenberg 2015), we assume that the source of gravitational waves is elliptically polarized so that the cross-polarized strain is completely determined by the plus-polarized strain:<sup>11</sup>

$$h_{\times}(f) = \epsilon h_{+}(f) e^{i\pi/2}. \quad (11)$$

Here,  $\epsilon \in [0, 1]$  is the ellipticity, which characterizes the polarization. We fit the binary black hole signal GW150914 using a superposition of sine-Gaussian wavelets; see Abbott (2016):

$$\Psi(t|A, f_0, t_0, \phi) = A e^{-(t-t_0)^2/\tau^2} \cos(2\pi f_0(t-t_0) + \phi) \quad (12)$$

with  $\tau = Q/(2\pi f_0)$ . Here,  $A$  is the amplitude,  $\tau$  is the damping time,  $Q$  is the quality factor,  $t_0$  is the central time,  $f_0$  is the central frequency, and  $\phi$  is the phase offset. The plus-polarized strain  $h_{+}$  is the summation of several components

$$h_{+}(t) = \sum_j \Psi(t|A_j, f_j, t_j, \tau_j, \phi_j). \quad (13)$$

We adopt the following priors: the amplitudes follow log uniform priors between  $[10^{-23}, 10^{-18}]$  and we constrain the amplitude for the  $(k+1)^{\text{th}}$  wavelet to be less than that of  $k^{\text{th}}$ . The quality factor  $Q$  is taken from a uniform distribution on the interval  $[2, 16]$ , and  $\phi$  follows a uniform distribution between 0 and  $2\pi$  with periodic boundary conditions.

For the  $k = 1$  wavelet, we adopt a uniform prior for  $f_0$  and  $t_0$ . For  $k > 1$ , we employ a proximity prior that require subsequent wavelets to be close to (but not too close to) the lower- $k$  wavelets. Following `BayesWave` (Cornish & Littenberg 2015), we employ two-dimensional, hollowed-out Gaussians in the  $f, t$  plane. For wavelet  $k$ , the prior is

$$\pi(t_k, f_k) = \sum_{i=1}^{k-1} \frac{\mathcal{N}_k}{k-1} \left( e^{-(f_k-f_i)^2/2\sigma_f^2} e^{-(t_k-t_i)^2/2\sigma_t^2} - e^{-(f_k-f_i)^2/2\beta^2\sigma_f^2} e^{-(t_k-t_i)^2/2\beta^2\sigma_t^2} \right).$$

<sup>10</sup> Strain data for GW150914 is accessed via Gravitational Wave Open Science Center (GWOSC) (LIGO Scientific Collaboration, Virgo Collaboration and KAGRA Collaboration 2018)

<sup>11</sup> For some bursting sources, it may be appropriate to adopt an unpolarized model so that  $h_{\times}$  is modelled independently from  $h_{+}$ .



Here,  $\mathcal{N}_k$  is a normalisation constant. The width of the Gaussians is controlled by variables  $\sigma_t$  and  $\sigma_f$ . The variable  $\beta$  controls the relative width of the hole in the middle of the Gaussian.<sup>12</sup> Following *BayesWave* (*Cornish & Littenberg 2015*), we adopt  $\beta = 0.25$ . As for the width of the Gaussian, we set  $\sigma_t = 0.8$  s and  $\sigma_f = 80$  Hz. One can change the values of  $\sigma_f$ ,  $\sigma_t$ , and  $\beta$  to adapt the model to different problems. However, these three variables are not treated as free parameters from the perspective of the sampler.

We analyze the LIGO–Virgo event GW150914 (*Abbott et al. 2016a*) using *dynesty* using the ghost parameter framework described above. We allow up to  $N_{\max} = 4$  wavelets (25 total parameters). We combine samples from several runs weighted by the evidence of each run (*Ashton & Khan 2020*). The sampling times range from 80 hrs to 210 hrs with 16 parallel processes running on a 3.0 GHz central processing unit. The reconstructed waveform is shown in Fig. 4 (red) alongside the whitened data (peach), and the compact binary coalescence (CBC) template fit shown as the blue curve.<sup>13</sup> The top panel is for the LIGO Hanford Observatory (LHO) while the bottom panel is for the LIGO Livingston Observatory (LLO). The wavelet fit produces a qualitatively similar reconstruction as the compact binary template fit. Both fits recover the morphology of key features in the whitened data. The wavelet fit produces a higher likelihood than the template fit ( $\Delta \ln \mathcal{L} = 4$ ). Since we expect the template derived from general relativity to fit the signal, we interpret this as evidence that the  $N = 4$  wavelet fit is beginning to overfit features in the noise.

The posterior strongly favours  $N = 4$  over  $N \leq 3$  with  $\gtrsim 99.99\%$  probability allocated to  $N = 4$ . This motivates extending our prior range to  $N_{\max} = 6$ . This follow-up test yields mixed results. On the one hand, some  $N = 6$  runs yield promising waveform reconstruction. On the other hand, the output is not stable run-to-run with current settings. This likely indicates that the sampler is failing to reliably converge for  $N = 6$ . In order to make further progress, it may be necessary to develop sampler settings that are better tuned for this transdimensional problem. We plan to adjust the im-

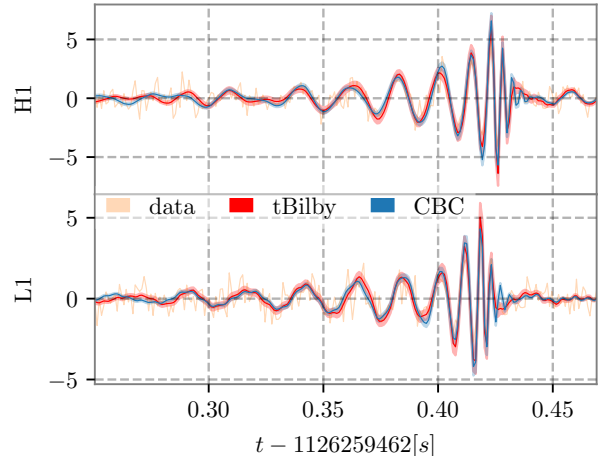


**Figure 4.** The reconstructed signal from GW150914. The red trace shows the signal reconstructed using a transdimensional sine-Gaussian wavelet fit. The blue trace shows the maximum-likelihood template obtained with the IMRPHENOMXPHM approximant. The whitened data is shown in peach. The top panel is for the H1 observatory in Hanford, WA while the bottom panel is for the L1 observatory in Livingston, LA.

plementation of *dynesty* in *tBilby* as a focus of future work.

In Fig. 5, we show the posterior distributions for the frequencies of  $N = 4$  wavelets. The blue posterior distributions are obtained with a fixed  $N = 4$  analysis using *Bilby*, while the orange results are obtained allowing for any value of  $N$  using *tBilby*. In Fig. 6 we show the sky localisation map for GW150914, where the blue curves are the 90% credible intervals obtained using the IMRPHENOMXPHM waveform approximant and the orange curves are obtained using our transdimensional sine-Gaussian wavelet fit.

#### 4. DISCUSSION AND CONCLUSIONS

We introduce the *tBilby* package that facilitates transdimensional inference calculations with *Bilby*. Focusing, to start with, on time-domain models with a superposition of component functions, we provide examples where users can employ off-the-shelf samplers in *Bilby* to reconstruct signals with minimal alterations. The package includes example implementations of ghost parameters and proximity priors, a useful ingredient for this class of transdimensional problems. We show how *tBilby* can be used to perform a minimum-assumption fit of GW150914 with sine-Gaussian wavelets as in *Abbott (2016)*.

For future work, we propose to improve the efficiency of *tBilby* through the use of more finely tuned sam-

<sup>12</sup> Here, we adopt a slightly different convention than *Cornish & Littenberg (2015)*. We employ a Gaussian of width  $\sigma$  hollowed out with a hole of width  $\beta\sigma$  while *Cornish & Littenberg (2015)* uses a Gaussian of width  $\alpha\sigma$  hollowed out with a hole of width  $\beta\sigma$ .

<sup>13</sup> The CBC fit is obtained using the waveform approximant IMRPHENOMXPHM (*Pratten et al. 2021*).

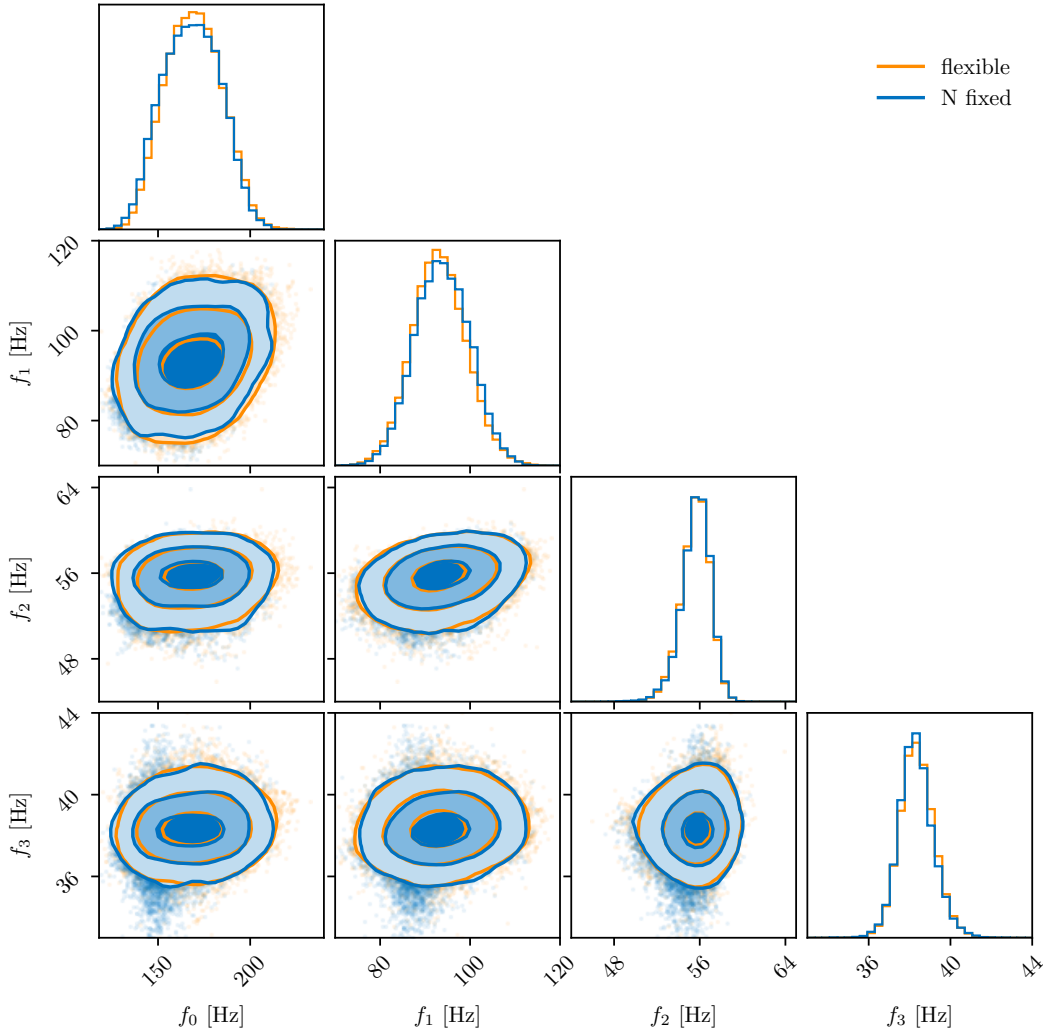


**Figure 5.** Posteriors for the frequencies of different sine-Gaussian wavelets fit to GW150914. The blue results are obtained with  $N = 4$  fixed. The orange shows posteriors of samples with  $N = 4$  from a transdimensional fit, which allows for any value of  $N$ .

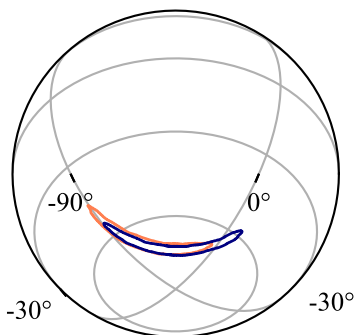


**Figure 6.** Sky map showing the 90 % credible intervals for GW150914 recovered by a compact binary coalescence template fit (blue) and a transdimensional sine-Gaussian wavelet fit (orange).

plers, designed for specific classes of problems of interest in gravitational-wave astronomy. Thanks to the modular design of `Bilby`, it is relatively easy to experiment with different options. While we find that `dynesty` produces well-converged fits to GW150914 for  $N_{\max} \leq 4$ , we do not obtain reliable fits with `ptemcee`—at least using the default settings. And even our `dynesty` runs are currently limited to  $N_{\max} = 4$  due to the scaling of the computational cost with  $N_{\max}$ . It may be necessary to employ custom jump proposals to improve convergence for `ptemcee` and/or to explore larger values of  $N_{\max}$ . Our work highlights the potential for carrying out transdimensional inference with nested sampling; see, e.g., [Brewer et al. \(2015\)](#).

We see this paper as the first step in a broader program to facilitate transdimensional inference with

Bilby—in gravitational-wave astronomy and other contexts. We highlight a few priorities. First, as evidenced by work done with `BayesLine` (Littenberg & Cornish 2015), transdimensional inference is a powerful tool for modelling the noise in gravitational-wave observatories; see also Gupta & Cornish (2023). Noise modelling naturally lends itself to transdimensional models because the noise power spectral density can be characterised by some fiducial shape plus a variable number of spectral features superposed on top. Transdimensional models can be used to obtain smooth fits of the noise power spectral density while characterizing instrumental lines and other features, enabling us to study the evolution of these features over the course of an observing run.

In Fig. 7, we show an example of a LIGO noise amplitude spectral density fit using `tBilby`. Inspired by Cahillane & Mansell (2022); Littenberg & Cornish (2015), our transdimensional model consists of a superposition of  $N$  power laws (to model broadband noise) and  $M$  Lorentzians (to model narrow lines). We analyze a 4s segment of data immediately preceding the GW150914 event. For illustrative purposes, we focus on a narrow frequency band between 450–550 Hz. (Work is ongoing to develop a model that reliably fits the entire LIGO observing band.) The transdimensional model (red) succeeds in fitting the data (peach) including several narrowband features. The posterior for  $N$  and  $M$  for this model peak at 4 and 7, respectively, even though the priors for these parameters extend up to 5 and 12, respectively. A comprehensive study will be detailed in a forthcoming publication. Code to reproduce this plot is available in the accompanying `asd.ipynb` notebook.

In terms of non-stationary noise modelling, we are also excited about the application of transdimensional sampling to model potential glitches simultaneously with compact binary signals (Chatziioannou et al. 2021a; Hourihane et al. 2022). This work may help astronomers to better interpret gravitational-wave events with potential data quality problems (Payne et al. 2022).

Second, we envision extending `tBilby` to build more flexible models describing the population properties of binary black holes and neutron stars; see, e.g., Toubiana et al. (2023). For example, one may wish to model the distribution of primary black hole mass mass distribution with a variable number of peaks and troughs. Recent studies have highlighted the usefulness of flexible models to identify structure that might be missing from astrophysically inspired phenomenological models; see, e.g., Tiwari & Fairhurst (2021); Edelman et al. (2022, 2023).

Finally, we propose to develop `tBilby` for applications beyond terrestrial gravitational-wave observato-

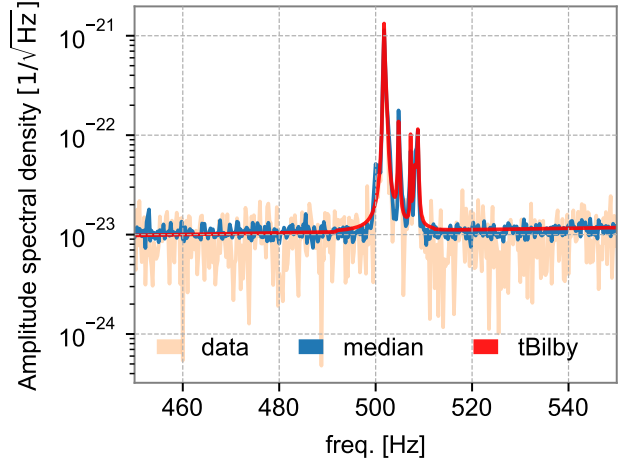


**Figure 7.** Fitting the noise amplitude spectral density in a narrow frequency band in the data before GW150914. The blue curve represents the median obtained using from 32 4s segments of data preceding GW150914. The red curve represents the maximum-likelihood estimation obtained from our `tBilby` model. The peach curve shows the 4s of data immediately preceding GW150914.

ries. For example, pulsar timing measurements, which can be used to measure nanohertz gravitational-waves (Agazie et al. 2023; Antoniadis et al. 2023; Reardon et al. 2023; Xu et al. 2023), rely on measurements of the time of arrival of arbitrarily shaped radio pulses. By modelling these pulses using a superposition of component functions, it is sometimes possible to identify and account for aberrant behaviour in the pulsar evolution, ultimately improving sensitivity for gravitational-wave searches (Nathan et al. 2023). Transdimensional models may prove useful determining the number of component functions used in these fits. Of course, this is just one example. It is our hope that the `tBilby` package will facilitate the development of numerous transdimensional models for physics and astronomy.



1 This work is supported through Australian Research  
 2 Council (ARC) Centre of Excellence CE170100004, Dis-  
 3 covery Projects DP220101610 and DP230103088, and  
 4 LIEF Project LE210100002. T. A. C. receives support  
 5 from the Australian Government Research Training Pro-  
 6 gram. The authors are grateful for for computational  
 7 resources provided by the LIGO Laboratory computing  
 8 cluster at California Institute of Technology supported  
 9 by National Science Foundation Grants PHY-0757058  
 10 and PHY-0823459, and the Ngarrgu Tindebeek / OzS-  
 11 TAR Australian national facility at Swinburne Univer-  
 12 sity of Technology. LIGO was constructed by the Cali-  
 13 fornia Institute of Technology and Massachusetts Insti-  
 14 tute of Technology with funding from the National Sci-  
 15 ence Foundation and operates under cooperative agree-  
 16 ment PHY-1764464. This paper carries LIGO Docu-  
 17 ment Number LIGO-P2400105.

## APPENDIX

### A. CODE DESIGN

The objective of `tBilby` is to provide a comprehensive toolkit for handling transdimensional sampling. The `tBilby` package offers flexibility and automation. As outlined in this Paper, the development of `tBilby` is part of a long-term project with multiple goals. At present, we have constrained the package to a set of essential tools and examples. `tBilby`'s design philosophy closely aligns with that of `Bilby`, emphasizing open-source code, modularity, generality, and usability (Ashton et al. 2019). Based on the ideas and infrastructure of `Bilby`, `tBilby` ensures a relatively smooth user experience, particularly for experienced users. Furthermore, we reinforce this philosophy by mandating that the sole requirement for `tBilby` is an installation of `Bilby`.

The structure of `tBilby` closely mirrors that of `Bilby`, with the core module including `base`, `prior`, and `sampler` modules, alongside an additional folder dedicated to examples. The `base` module contains fundamental functionality for constructing transdimensional models and defining transdimensional priors. The `prior` folder houses priors intended for transdimensional sampling, while the `sampler` module facilitates support for transdimensional samplers.

The key building block of a transdimensional model in `tBilby` is the *transdimensional parameter*, which refers to a parameter of a component function that has multiple “orders” (in this language, each sine-Gaussian is a different order). Another fundamental concept is the *transdimensional prior*, which constitutes a set of priors related to a transdimensional parameter and which is attached to the parameter’s order. Transdimensional models with proximity priors employ conditional statements. These two elements serve as the basic building blocks.

For practical purposes, transdimensional priors in `tBilby` are categorized into four types: (i) transdimensional nested conditional priors, (ii) transdimensional conditional priors, (iii) conditional priors, and (iv) unconditional priors.<sup>14</sup> Transdimensional nested conditional priors are defined by their dependence on previously sampled parameters of the same component function. If we assume that the current order being sampled is  $n$ , these priors depend on parameters of orders  $n - 1$ ,  $n - 2$ , etc.

Transdimensional conditional priors, on the other hand, are dependent on parameters from all sampled orders of a component function, denoted by  $k, k - 1$ , etc. Conditional priors rely on a set of non-transdimensional parameters, whereas unconditional priors are independent of other parameters. The most general prior may combine elements of all these types, except for the last type, which by definition is an independent prior. In this framework, the most

<sup>14</sup> Examples employing each of the prior types can be found at the `git` repository.

general form of a prior for transdimensional parameter  $\rho_n$  is:

$$\pi(\rho_n | \rho_{n-1}, \dots, \phi_{n-1}, \dots, \zeta_k, \zeta_{k-1}, \dots, \Lambda).$$

The variable  $\phi$  represents another set of transdimensional parameters of the same order as the component function so that  $\rho_n$  does not depend on  $\phi_{m \geq n}$ . Meanwhile,  $\zeta$  signifies another set of transdimensional parameters that depend on all available orders of the component function. Finally,  $\Lambda$  are parameters that may or may not be part of the component function parameters.

By allowing for the definition of conditional transdimensional priors, users can uniquely specify priors for each transdimensional parameter. Practically, this involves defining a class that inherits from a predefined transdimensional prior class and implementing an abstract function to define the mathematical relation between the conditional parameters and prior properties (this is a generalization of `Bilby`'s condition function, which is required when defining a conditional prior).

Facilitating such versatility and control over the priors allows users to gain flexibility in manipulating the prior distribution to suit their specific needs. The flexibility of `tBilby`'s extends further, enabling the construction of function superposition, each potentially comprising a different number of component functions. For instance, the LIGO noise power spectral density may be represented as a combination of several power law functions along with multiple Cauchy-like functions, addressing distinct spectral characteristics (Littenberg & Cornish 2015). Furthermore, `tBilby` offers supplementary tools for removing ghost parameters and generating relevant corner plots, thereby simplifying the analysis of component functions and individual transdimensional parameters.

## B. GHOST PARAMETER

The method outlined here is similar to Liu et al. (2023) who performed transdimensional inference using `Bilby` for gravitational-wave lensing study. In the ghost parameter framework, we introduce extra parameters that do not actually change the likelihood, and therefore do not change the posteriors for the original parameters—as long as the ghost-parameter prior is correctly normalized. For example, we consider the situation in Section 3.1 when  $N = 3$ . The signal is only determined by  $\theta_{k \leq 3}$  while  $\theta'_{k > 3}$  represents the ghost parameters. In this case, the posterior is

$$p(\theta_{k \leq 3}, \theta_{k > 3}, N = 3 | d) = p(\theta_{k \leq 3}, \theta_{k > 3} | d, N = 3) p(N = 3 | d). \quad (\text{B1})$$

The conditional posterior given  $N$  can be written as

$$p(\theta_{k \leq 3}, \theta_{k > 3} | d, N = 3) = \frac{\mathcal{L}(d | \theta_{k \leq 3}) \pi(\theta_{k \leq 3}) \pi(\theta_{k > 3} | \theta_{k \leq 3})}{p(N = 3 | d) / \pi(N = 3)}. \quad (\text{B2})$$

As the priors for the extra parameters are properly normalized by definition, i.e.,

$$\int p(\theta'_{k > 3} | \theta_{k \leq 3}) d\theta'_{k > 3} = 1, \quad (\text{B3})$$

the marginalized posterior for  $\theta_{k \leq 3}$  is equivalent to the case where there are no extra parameters:

$$\begin{aligned} p(\theta_{k \leq 3} | d, N = 3) &\propto \int \mathcal{L}(d | \theta_{k \leq 3}) \pi(\theta_{k \leq 3}) \pi(\theta_{k > 3} | \theta_{k \leq 3}) d\theta_{k > 3} \\ &\propto \mathcal{L}(d | \theta_{k \leq 3}) \pi(\theta_{k \leq 3}). \end{aligned} \quad (\text{B4})$$

Now we take a look at the denominator of Eq. B2. It is actually the marginal likelihood of  $N$  in transdimensional sampling:

$$\mathcal{L}(d | N = 3) = p(N = 3 | d) / \pi(N = 3). \quad (\text{B5})$$

Meanwhile, we note it is essentially a normalization factor, so the expression can be also written as

$$\begin{aligned} \mathcal{L}(d | N = 3) &= \int \mathcal{L}(d | N = 3, \theta_{k \leq 3}) \times \\ &\quad \pi(\theta_{k \leq 3}) \pi(\theta'_{k > 3} | \theta_{k \leq 3}) d\theta_{k \leq 3} d\theta_{k > 3} \\ &= \int \mathcal{L}(d | \theta_{k \leq 3}) \pi(\theta_{k \leq 3}) d\theta_{k \leq 3} \\ &= \mathcal{Z}_{N=3}. \end{aligned} \quad (\text{B6})$$

We make use of the fact that the priors for ghost parameters are properly normalized again.

So the model selection result of our transdimensional problem with ghost parameters is valid regardless of the inclusion of ghost parameters as the likelihood  $\mathcal{L}(d|N=3)$  is correctly defined as the case without the implementation of ghost parameters.

As a comparison, the detailed balance equations of traditional reversible jump Markov chain Monte Carlo without ghost parameters is written as

$$p(\theta_{k \leq 3}|d)q(\theta'_{k \leq 3}, \theta'_{k > 3}) = p(\theta'_{k \leq 3}, \theta'_{k > 3}|d)q(\theta_{k \leq 3})\alpha, \quad (\text{B7})$$

where  $p(\theta|d)$  is the target distribution, i.e., posteriors in Bayesian inference,  $q(\theta)$  is the proposal for samples in Markov chain Monte Carlo sampling and  $\alpha$  is the acceptance probability. This makes use of the trade-off between higher dimension proposals in the left-hand side and higher dimension posteriors in the right-hand side.

With the implementation of ghost parameters, we artificially add extra dimensions for posteriors and proposals in both side with the detailed balance equation written as

$$p(\theta_{k \leq 3}, \theta_{k > 3}|d)q(\theta'_{k \leq 3}, \theta'_{k > 3}) = p(\theta'_{k \leq 3}, \theta'_{k > 3}|d)q(\theta_{k \leq 3}, \theta_{k > 3})\alpha. \quad (\text{B8})$$

As we show above, in the case where  $\theta_{k > 3}$  are not used in the evaluation of the likelihood, the posteriors could be written as two independent parts

$$p(\theta_{k \leq 3}, \theta_{k > 3}|d) = p(\theta_{k \leq 3}|d) \times \pi(\theta'_{k > 3}|\theta_{k \leq 3}). \quad (\text{B9})$$

Thus, if we choose a proper reversible proposal distribution to make

$$\begin{aligned} q(\theta'_{k \leq 3}, \theta'_{k > 3}) &= q(\theta'_{k \leq 3})q(\theta'_{k > 3}|\theta'_{k \leq 3}) \\ &= q(\theta'_{k \leq 3})\pi(\theta_{k > 3}|\theta_{k \leq 3}), \end{aligned}$$

then the detailed balance can be written as

$$\begin{aligned} p(\theta_{k \leq 3}|d)\pi(\theta_{k > 3}|\theta_{k \leq 3})q(\theta'_{k \leq 3}, \theta'_{k > 3}) &= \\ p(\theta'_{k \leq 3}, \theta'_{k > 3}|d)q(\theta'_{k \leq 3})\pi(\theta_{k > 3}|\theta_{k \leq 3})\alpha. & \end{aligned} \quad (\text{B10})$$

This reduces to Eq.B7 where we do not implement ghost parameters. In fact, it is not necessary to set up special proposals for ghost parameters. With arbitrary proposal distributions, the sampling result with the implementation of ghost parameters will always be consistent with the situation without ghost parameters as the statistical average of acceptance rate  $\alpha$  over the entire parameters space.

## REFERENCES

- Aasi, J., et al. 2015, *Class. Quant. Grav.*, 32, 074001
- Abbott, B. P. 2016, *Phys. Rev. D*, 93, 122004
- Abbott, B. P., et al. 2016a, *Phys. Rev. Lett.*, 116, 061102
- . 2016b, *Phys. Rev. Lett.*, 116, 241102
- . 2016c, *Phys. Rev. Lett.*, 116, 221101
- . 2017, *Nature*, 551, 85
- . 2018, *Phys. Rev. Lett.*, 121, 161101
- Abbott, R., et al. 2021, *Astrophys. J. Lett.*, 913, L7
- . 2023, *Phys. Rev. X*, 13, 011048
- Acernese, F., et al. 2015, *Class. Quant. Grav.*, 32, 024001
- Agazie, G., et al. 2023, *Astrophys. J. Lett.*, 956, L3
- Antoniadis, J., et al. 2023, *Astron. Astrophys.*, 678, A50
- Ashton, G., & Dietrich, T. 2022, *Nature Astronomy*, 6, 961
- Ashton, G., & Khan, S. 2020, *Physical Review D*, 101, 064037
- Ashton, G., et al. 2019, *Astrophys. J. Supp.*, 241, 27
- Aso, Y., Michimura, Y., Somiya, K., et al. 2013, *Phys. Rev. D*, 88, 043007
- Brewer, B. J., Huijser, D., & Lewis, G. F. 2015, *Mon. Not. R. Ast. Soc.*, 455, 1819
- Cahillane, C., & Mansell, G. 2022, *Galaxies*, 10, 36, doi: [10.3390/galaxies10010036](https://doi.org/10.3390/galaxies10010036)
- Chatziioannou, K., Cornish, N., Wijngaarden, M., & Littenberg, T. B. 2021a, *Physical Review D*, 103, 044013
- Chatziioannou, K., Isi, M., Haster, C.-J., & Littenberg, T. B. 2021b, *Phys. Rev. D*, 104, 044005

- Cornish, N. J., & Littenberg, T. B. 2015, *Class. Quantum Grav.*, 32, 135012
- Cornish, N. J., Littenberg, T. B., Bècsy, B., et al. 2021, *Phys. Rev. D*, 103, 044006
- Dàlya, G., Raffai, P., & Bècsy, B. 2021, Bayesian reconstruction of gravitational-wave signals from binary black holes with nonzero eccentricities
- Davis, D., Littenberg, T. B., Romero-Shaw, I. M., et al. 2022, *Class. Quantum Grav.*, 39, 245013
- Edelman, B., Doctor, Z., Godfrey, J., & Farr, B. 2022, *Astrophys. J.*, 924, 101
- Edelman, B., Farr, B., & Doctor, Z. 2023, *Astrophys. J.*, 946, 16
- Ellis, J., & Cornish, N. 2016, *Phys. Rev. D*, 93, 084048
- Green, P. J. 1995, *Biometrika*, 82, 711
- Gupta, T., & Cornish, N. 2023, *Phys. Rev. D*, 109, 064040
- Hotokezaka, K., Nakar, E., Gottlieb, O., et al. 2019, *Nature*, 3, 940
- Hourihane, S., Chatzioannou, K., Wijngaarden, M., et al. 2022, *Physical Review D*, 106, 042006
- Johnson-McDaniel, N. K., Ghosh, A., Ghonge, S., et al. 2022, *Phys. Rev. D*, 105, 044020
- Karnesis, N., Katz, M. L., Korsakova, N., Gair, J. R., & Stergioulas, N. 2023, Eryn: A multi-purpose sampler for Bayesian inference
- Klimenko, S., Yakushin, I., Mercer, A., & Mitselmakher, G. 2008, *Class. Quantum Grav.*, 25, 114029
- Kronland-Martinet, R., Morlet, J., & Grossmann, A. 1987, *International Journal of Pattern Recognition and Artificial Intelligence*, 1, 273
- LIGO Scientific Collaboration, Virgo Collaboration and KAGRA Collaboration. 2018, GWTC-1 Data Release, <https://gwosc.org/GWTC-1/>
- Littenberg, T., Cornish, N., Lackeos, K., & Robson, T. 2020, *Phys. Rev. D*, 101, 123021
- Littenberg, T. B., & Cornish, N. J. 2010, *Phys. Rev. D*, 82, 103007
- . 2015, *Phys. Rev. D*, 91, 084034
- Littenberg, T. B., Kanner, J. B., Cornish, N. J., & Millhouse, M. 2016, *Phys. Rev. D*, 94, 044050
- Liu, A., Wong, I. C. F., Leong, S. H. W., et al. 2023, *Monthly Notices of the Royal Astronomical Society*, 525, 4149
- Millhouse, M., Cornish, N. J., & Littenberg, T. 2018, *Phys. Rev. D*, 97, 104057
- Miravet-Tenés, M., Florencia L. Castillo, R. D. P., Cerdá-Durán, P., & Font, J. A. 2023, *Phys. Rev. D*, 107, 103053
- Nathan, R. S., et al. 2023, *Mon. Not. R. Ast. Soc.*, 523, 4405
- Pankow, C., et al. 2018, *Phys. Rev. D*, 98, 084016
- Pannarale, F., Macas1, R., & Sutton, P. J. 2021, *Class. Quantum Grav.*, 36, 035011
- Payne, E., Hourihane, S., Golomb, J., et al. 2022, *Phys. Rev. D*, 106, 104017
- Pratten, G., et al. 2021, *Phys. Rev. D*, 103, 104056
- Raza, N., McIver, J., Dàlya, G., & Raffai, P. 2022, *Phys. Rev. D*, 106, 063014
- Reardon, D. J., et al. 2023, *Astrophys. J. Lett.*, 951, L6
- Romero-Shaw, I. M., et al. 2020, *Mon. Not. R. Ast. Soc.*, 499, 3295
- Speagle, J. S. 2020, *Mon. Not. R. Ast. Soc.*, 493, 3132
- Tiwari, V., & Fairhurst, S. 2021, *Astrophys. J. Lett.*, 913, L19
- Toubiana, A., Katz, M. L., & Gair, J. R. 2023, *Mon. Not. R. Ast. Soc.*, 524, 5844
- Vousden, W. D., Farr, W. M., & Mandel, I. 2015, *mnras*, 455, 1919
- Xu, H., et al. 2023, *Res. Astrono. Astrophys.*, 23, 075024
- Yi Shuen C. Lee, M. M., & Melatos, A. 2021, *Phys. Rev. D*, 103, 062002